

## SYNTHESIS, CRYSTAL STRUCTURE, AND LUMINESCENCE OF THE ONE- DIMENSIONAL LANTHANUM(III) COORDINATION POLYMER WITH 2,6-BIS (3,5-DICARBOXYPHENOXY)PYRIDINE

X.-L. Yu<sup>1,2</sup>, D. I. Pavlov<sup>1</sup>, A. A. Ryadun<sup>1</sup>,  
A. S. Potapov<sup>1\*</sup>, and V. P. Fedin<sup>1,2</sup>

By the interaction of 2,6-bis(3,5-dicarboxyphenoxy)pyridine (H<sub>4</sub>L) with lanthanum(III) nitrate in a 1:1 acetonitrile–water mixture a coordination polymer {[La(HL)(H<sub>4</sub>L)(H<sub>2</sub>O)<sub>4</sub>]·2H<sub>2</sub>O}<sub>n</sub> is synthesized. According to single crystal X-ray diffraction data, the compound is a linear coordination polymer whose chains are organized into a 3D supramolecular network by  $\pi$ – $\pi$  stacking interactions and hydrogen bonds. The coordination polymer exhibits intraligand luminescence with the emission maximum at 392 nm.

DOI: 10.1134/S0022476622120149

**Keywords:** lanthanum, carboxylate ligands, metal-organic frameworks, crystal structure, single crystal X-ray diffraction analysis, photoluminescence.

### INTRODUCTION

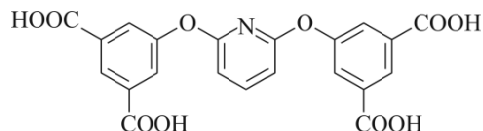
After the first examples of metal-organic frameworks (MOFs) have been obtained, they continue to attract the researchers' interest due to their ability to selective gas and vapor adsorption [1, 2], luminescent [3, 4] and catalytic properties [5, 6]. More and more new types of organic ligands – MOF building blocks – are introduced in the synthesis practice [7]. One of these types are aromatic polycarboxylic acids, which additionally contain ether bridges imparting conformational mobility to the ligands [8-10]. The presence of several carboxyl groups in different electronic and steric environments often results in that some of them remain in the protonated form after the MOF formation and are not involved in coordination by metal ions. Due to their acidity, high polarity, and binding capability of both organic compounds and metal ions, free carboxyl groups in the MOF composition noticeably change their properties enhancing the proton conductivity, increasing the gas adsorption selectivity or catalytic transformations [11]. The nature of the metal ion is no less important for the MOF properties. Lanthanide ions are able to form many strong coordination bonds with oxygen atoms in polycarboxylate ligands, which increases the hydrolytic and thermal stability of resulting MOFs. Among all lanthanides whose ions can be included in the MOF structure, in the literature, the most attention is paid to europium(III) and terbium(III), primarily due to their specific luminescent properties [12]. Despite its much greater availability, lanthanum(III) is far less common as a complexing agent,

---

<sup>1</sup>Nikolaev Institute of Inorganic Chemistry, Siberian Branch, Russian Academy of Sciences, Novosibirsk, Russia; \*potapov@niic.nsc.ru. <sup>2</sup>Novosibirsk State University, Novosibirsk, Russia. Original article submitted October 18, 2022; revised October 19, 2022; accepted October 19, 2022.

however, in this case, synthesized MOFs also exhibit potentially useful properties, such as the ability to extract anions from aqueous solutions [13-15] or to gas absorption [16].

The work studies the interaction of lanthanum(III) nitrate and the tetracarboxylate ligand with flexible ether bridges of 2,6-bis(3,5-dicarboxyphenoxy)pyridine (Scheme 1). To date, only one coordination polymer based on this ligand and copper(II) ions has been described in the literature [17], and there is no information about the possibility to obtain coordination compounds with other metal ions.



**Scheme 1.** Structure of 2,6-bis(3,5-dicarboxyphenoxy)pyridine.

## EXPERIMENTAL

All reagents used in the work were at least of analytical grade and were used without further purification. 2,6-Bis(3,5-dicarboxyphenoxy)pyridine ( $H_4L$ ) was purchased from Jinan Henghua Sci. & Tec. Co. Ltd. (Jinan, PRP).

The XRD patterns of powder samples were recorded on a Bruker D8 ADVANCE diffractometer,  $CuK_{\alpha}$  radiation,  $\lambda = 1.5406 \text{ \AA}$ ,  $2\theta$  range of  $3-40^\circ$ . The elemental analysis was performed on a Vario MICRO Cube analyzer. The thermogravimetric analysis was carried out on a NETZSCH TG 209 F1 Iris Thermo Microbalance in the helium atmosphere in a temperature range of  $30-850^\circ\text{C}$ , heating rate  $10^\circ\text{C}/\text{min}$ . The IR absorption spectra were measured on a VERTEX 80 Fourier spectrometer in KBr pellets in a range of  $4000-400 \text{ cm}^{-1}$ . The emission and excitation spectra, photoluminescence decay kinetics were recorded on a Fluorolog-3 spectrofluorimeter (Horiba Jobin Yvon) with a cooled PC177CE-010 photon detection module equipped with an R2658 photo-multiplier and a time-correlated single photon counting system.

The crystallographic data for compound **1** were obtained at 140 K on an automated Agilent Xcalibur diffractometer with a two-dimensional AtlasS2 detector (graphite monochromator,  $\lambda(\text{Mo}K_{\alpha}) = 0.71073 \text{ \AA}$ ,  $\omega$ -scanning with a step of  $0.5^\circ$ ). Integration was performed, absorption corrections were applied, and unit cell parameters were determined using the CrysAlisPro software [18]. The crystal structures were solved and refined by full-matrix LSM in the anisotropic (except for hydrogen atoms) approximation using the Olex2 software [19]. The crystallographic data and details of the diffraction experiment are given in Table 1. Full tables of interatomic distances and bond angles, atomic coordinates and displacement parameters have been deposited with the Cambridge Crystallography Data Center (CCDC 2211564) and are available from the authors.

**Synthesis of compound  $\{[\text{La}(\text{HL})(\text{H}_4\text{L})(\text{H}_2\text{O})_4]\cdot 2\text{H}_2\text{O}\}_n$  (**1**).** To tetracarboxylic acid  $H_4L$  (4.6 mg, 0.0114 mmol) and  $\text{La}(\text{NO}_3)_3\cdot 6\text{H}_2\text{O}$  (6.6 mg, 0.0152 mmol) 2 mL of a mixture of acetonitrile–water solvents in 1:1 (vol.) were added. The suspension was magnetically stirred for 5 min at room temperature, transferred into a glass ampoule, sealed, and kept for 48 h at  $120^\circ\text{C}$ . The crystals formed were decanted and washed with a 1:1 acetonitrile–water mixture. Yield: 3.9 mg (60% per  $H_4L$ ), colorless crystals. IR spectrum (KBr),  $\nu$ ,  $\text{cm}^{-1}$ : 1690 m, 1584 m, 1549 m, 1532 s, 1439 w, 1397 w, 1294 w, 1221 w, 1065 s, 1024 m, 768 w, 710 w, 687 w. Found (%): C 44.2, H 3.3, N 2.5. Calculated for  $\text{C}_{42}\text{H}_{35}\text{N}_2\text{O}_{26}\text{La}$  (%): C 44.9, H 3.1, N 2.5.

**TABLE 1.** Crystallographic Parameters and Details of the Diffraction Experiment for Compound **1**

Parameter	<b>1</b>
Chemical formula	C <sub>42</sub> H <sub>35</sub> N <sub>2</sub> O <sub>26</sub> La
Molecular weight	2171.74
Temperature, K	140(2)
Crystal system	Triclinic
Space group	<i>P</i> $\bar{1}$
<i>a</i> , <i>b</i> , <i>c</i> , Å	8.5563(2), 13.8338(3), 19.1769(4)
$\alpha$ , $\beta$ , $\gamma$ , deg	76.942(2), 82.782(2), 80.519(2)
<i>V</i> , Å <sup>3</sup>	2171.74(9)
<i>Z</i>	2
$\rho_{\text{calc}}$ , g/cm <sup>3</sup>	1.717
$\mu$ , mm <sup>-1</sup>	1.086
<i>F</i> (000)	1132.0
Crystal size, mm	0.29×0.14×0.04
$\theta$ scanning range, deg	2.20–28.8
Reflection index ranges	$-11 \leq h \leq 11$ , $-18 \leq k \leq 18$ , $-26 \leq l \leq 20$
Measured reflections	20349
Independent reflections	9725
Reflections with $I > 2\sigma(I)$	0.0281
$R_{\text{int}}$	8788
<i>GOOF</i>	1.112
<i>R</i> factors ( $I > 2\sigma(I)$ )	$R_1 = 0.0350$ , $wR_2 = 0.0753$
<i>R</i> factors (all reflections)	$R_1 = 0.0414$ , $wR_2 = 0.0782$
Residual electron density (max / min), e/Å <sup>3</sup>	0.81 / -0.67

## RESULTS AND DISCUSSION

Compound **1** was prepared by the interaction of lanthanum(III) nitrate and proligand tetracarboxylic acid H<sub>4</sub>L in an acetonitrile–water (1:1) mixture under solvothermal conditions at 120 °C. The reaction conditions were optimized to obtain the reaction product in the form of single crystals suitable for the XRD analysis.

According to single crystal XRD, compound **1** crystallizes in the triclinic crystal system, space group *P* $\bar{1}$ . The asymmetric unit includes one La<sup>3+</sup> ion and two forms of the ligand (partially deprotonated (HL<sup>3-</sup>) and neutral (H<sub>4</sub>L)), as well as four coordinated and two solvate water molecules (Fig. 1*a*). The coordination number of the La<sup>3+</sup> ion is nine; it coordinates one neutral H<sub>4</sub>L molecule through one oxygen atom of the carboxyl group and three HL<sup>3-</sup> anions, with monodentate coordination of the carboxylate group for two of them and bidentate coordination for one of them being observed. The other four coordination sites are occupied by water molecules. In general, according to the estimation using the Shape 2.1 software [20], the coordination polyhedron is best described by a muffin (MFF) shape [21] (Fig. 1*b*). The La–O bond lengths are in a range from 2.486(2) Å to 2.7316(19) Å, which is typical of coordination lanthanum compounds with carboxylate ligands [22–24].

In the crystal structure of compound **1**, each La<sup>3+</sup> ion is linked by bridging HL<sup>3-</sup> anions with two other La<sup>3+</sup> cations into chains of a 1D coordination polymer oriented along the *a* crystallographic axis (Fig. 1*c*, *d*). These chains are packed into layers by hydrogen bonds formed with the participation of carboxyl groups of neutral H<sub>4</sub>L ligands; the layers are parallel to the *ab* plane (Fig. 1*e*). The geometric parameters of hydrogen bonds are given in Table 2. Due to  $\pi$ – $\pi$ -stacking interactions

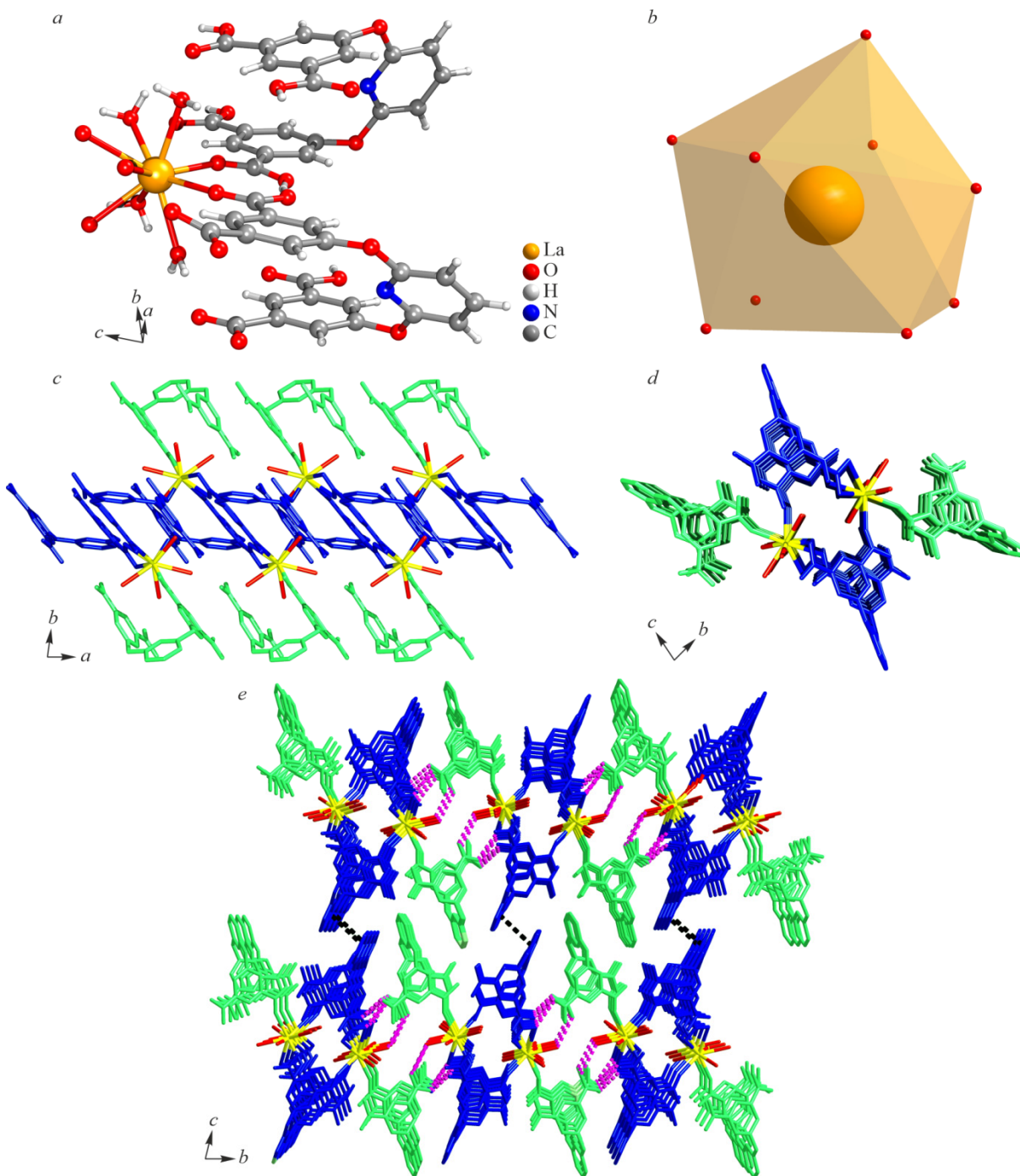


**Fig. 1.** Structure of coordination polymer **1** according to the single crystal XRD data: the structure of the asymmetric unit (*a*); the coordination polyhedron of the  $\text{La}^{3+}$  ion (*b*); the view of linear chains of the coordination polymer along the *c* and *a* axes; deprotonated ligands ( $\text{HL}^{3-}$ ) are shown by blue (see the electronic version), protonated ligands ( $\text{H}_4\text{L}$ ) are shown by green (*c*, *d*); the 3D supramolecular structure of the coordination polymer;  $\pi$ - $\pi$ -stacking interactions are shown by black dashed lines, hydrogen bonds are shown by violet dashed lines (*e*).

between pyridine rings located in parallel planes at a distance of 3.570 Å, the layers are packed into a 3D supramolecular structure (Fig. 1*e*).

Inside the building block of the coordination polymer there is also one  $\text{O19-H}\cdots\text{O17}$  hydrogen bond between two coordinated carboxyl groups of two different ligands:  $\text{HL}^{3-}$  and  $\text{H}_4\text{L}$  (Fig. 2, Table 2). It should be noted that this coordination mode of protonated and deprotonated carboxyl groups with the formation of the hydrogen bond between them is sufficiently

**TABLE 2.** Geometric Parameters of Hydrogen Bonds in the Structure of Compound **1**

Bond	$D\cdots A$ distance, Å	$D-H\cdots A$ angle, deg
O4-H $\cdots$ O15	2.618(3)	165
O6-H $\cdots$ O16	2.551(3)	171
O21-H $\cdots$ O23	2.969(4)	145
O19-H $\cdots$ O17	2.401(3)	170

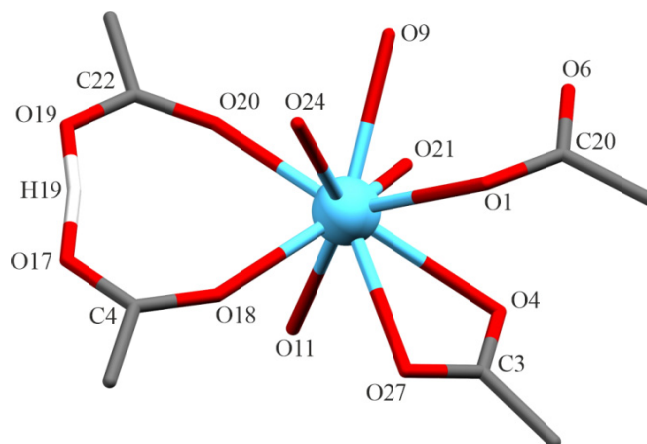


**Fig. 2.** Coordination of carboxyl and carboxylate groups by the  $\text{La}^{3+}$  ion in compound **1** with the formation of the O19–H $\cdots$ O17 hydrogen bond. To simplify the figure, only carbon atoms of COO groups are shown, hydrogen atoms are omitted.

rare and has been previously observed only in six coordination compounds of copper(II) [25], magnesium(II) [26], manganese(II) [27] and in three isostructural carboxylate complexes of praseodymium(III), neodymium(III), and lanthanum(III) [28]. In the latter case, the distance between the oxygen atoms sharing a proton (2.475(2) Å) is similar to that in compound **1**.

The phase purity of compound **1** was confirmed by powder XRD. As can be seen from Fig. 3a, each peak in the experimental XRD pattern of the powder sample corresponds to each peak calculated from the single crystal XRD data for

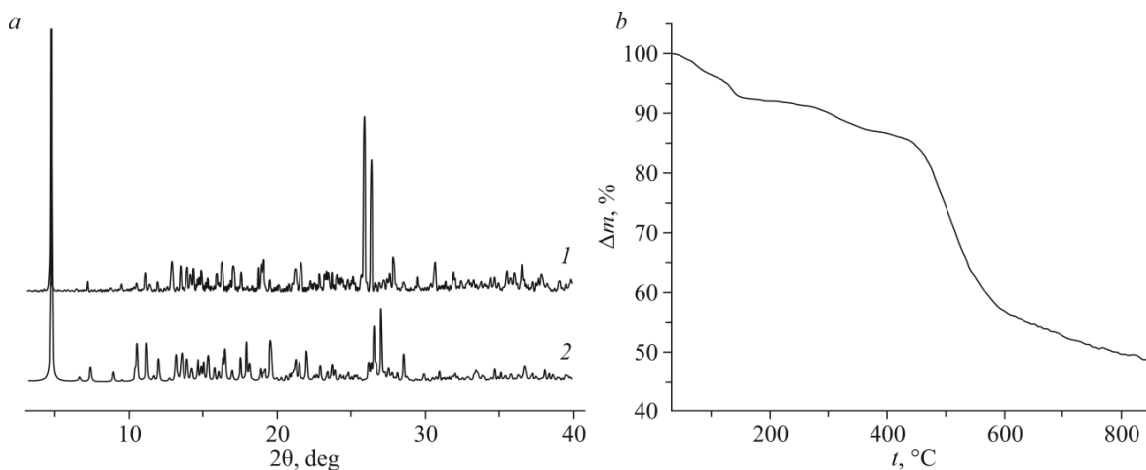


**Fig. 3.** Experimental (1) and calculated (2) powder XRD patterns of compound **1** (a); the thermogravimetric curve of compound **1** (b).

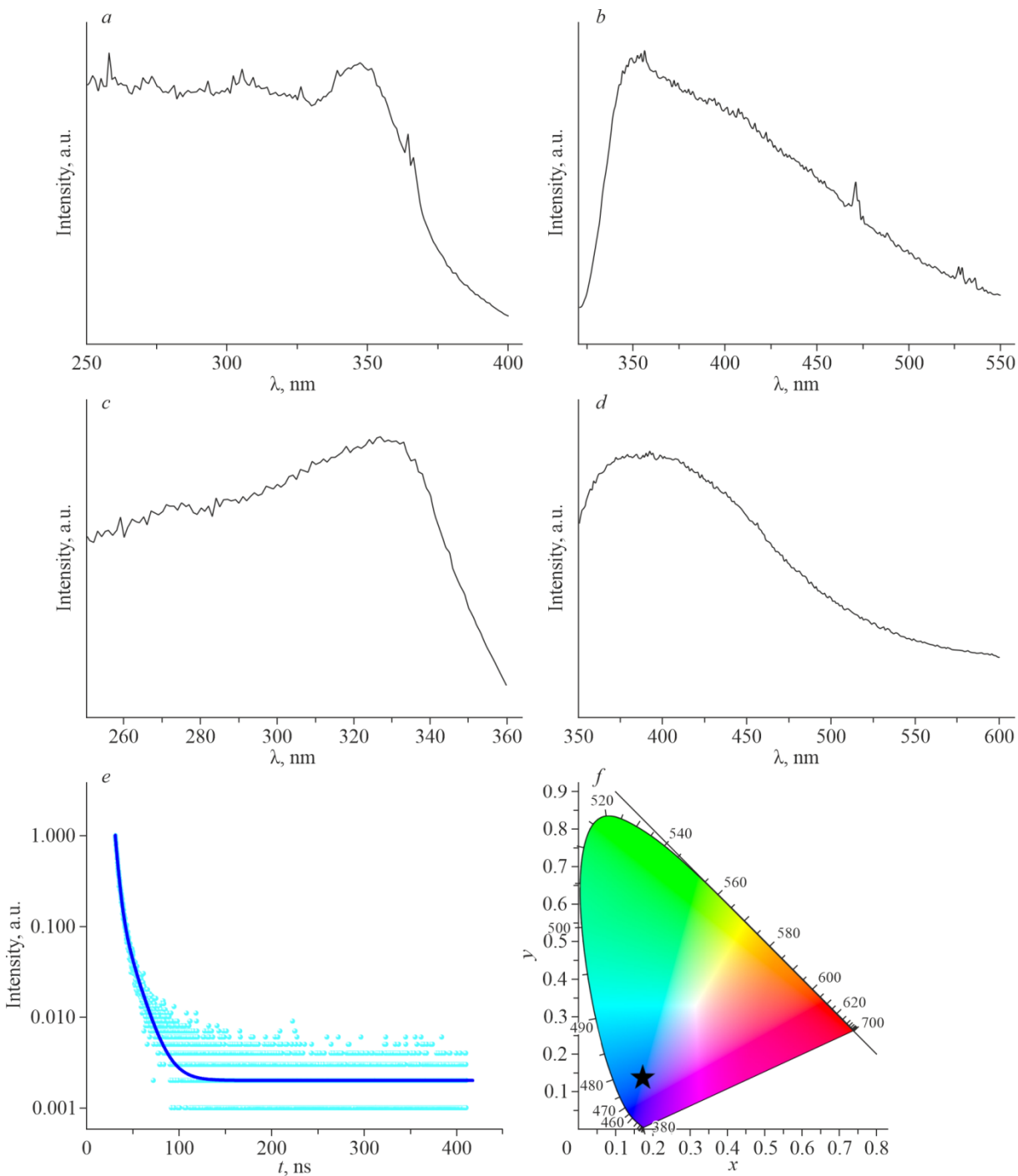


**Fig. 4.** Photoluminescence excitation and emission spectra of the H<sub>4</sub>L proligand in the solid phase (*a, b*); the photoluminescence excitation and emission spectra of coordination polymer **1** in the solid phase (*c, d*); the luminescence decay curve of coordination polymer **1** (*e*); the CIE-1931 chromaticity diagram with the point corresponding to emission of compound **1** (*f*).

compound **1**, while the peaks of other phases were not detected. The results of the (CHN) elemental analysis confirm that the product is chemically pure and its chemical formula corresponds to the single crystal XRD data.

According to the thermogravimetric data (Fig. 3*b*), the loss of solvate water molecules starts almost immediately after the onset of heating and ends at a temperature of about 100 °C (weight loss 3.6%, calculated for two water molecules 3.2%). Right after this, the loss of four coordinated water molecules begins, which ends at about 290 °C (weight loss 9.5%,

calculated for six water molecules 9.6%). Above this temperature, the organic ligand in the composition of the coordination polymer begins to decompose.

The luminescent properties of coordination polymer **1** and the proligand H<sub>4</sub>L were studied in the solid phase at room temperature. When excited at a wavelength of 347 nm, tetracarboxylic acid H<sub>4</sub>L exhibits broadband emission with the maximum near 356 nm (Fig. 4a, b) due to  $\pi \rightarrow \pi^*$  transitions in the aromatic system of the organic compound. The spectra of compound **1** have a bathochromic shift of the emission band with the maximum near 392 nm and a hypsochromic shift of the absorption band with the maximum near 327 nm (Fig. 4c, d). The luminescence decay kinetics of compound **1** at room temperature (Fig. 4e) can be described by the monoexponential dependence  $I = A_0 + A \exp(-t/\tau)$ . The calculated luminescence lifetime  $\tau$  is 3 ns; the nanosecond time range is indicative of the intraligand nature of fluorescence. The color coordinates determined from the emission spectrum of compound **1** are (0.1722, 0.1351) and correspond to cool blue (Fig. 4f).

## CONCLUSIONS

Thus, the first example of a coordination compound of rare-earth elements with a poorly studied organic proligand 2,6-bis(3,5-dicarboxyphenoxy)pyridine was synthesized and characterized by conventional methods. According to the single crystal XRD data, the compound is a chain coordination polymer with a 3D supramolecular structure formed via hydrogen bonds and  $\pi$ - $\pi$  stacking. The presence of a ligand molecule with four protonated carboxyl groups in the structure of the coordination polymer suggests the possibility to obtain higher dimensional (two- and three-dimensional) coordination polymers and prospects for the further research of other lanthanides.

## FUNDING

The work was supported by the Ministry of Science and Higher Education of the Russian Federation (Projects Nos. 121031700321-3 and 121031700313-8).

## ACKNOWLEDGMENTS

Xiaolin Yu is grateful to the China Scholarship Council for financial support (Grant No. 202008090088).

## CONFLICT OF INTERESTS

The authors declare that they have no conflicts of interests.

## REFERENCES

1. K. A. Kovalenko, A. S. Potapov, and V. P. Fedin. *Russ. Chem. Rev.*, **2022**, *91*, RCR5026. <https://doi.org/10.1070/RCR5026>
2. Y. G. Gorbunova, Y. Y. Enakieva, M. V. Volostnykh, A. A. Sinelshchikova, I. A. Abdulaeva, K. P. Birin, and A. Yu. Tsivadze. *Russ. Chem. Rev.*, **2022**, *91*, RCR5038. <https://doi.org/10.1070/rcr5038>
3. Y. Liu, X.-Y. Xie, C. Cheng, Z.-S. Shao, and H.-S. Wang. *J. Mater. Chem. C*, **2019**, *7*, 10743. <https://doi.org/10.1039/C9TC03208H>
4. A. Kuznetsova, V. Matveevskaya, D. Pavlov, A. Yakunenkov, and A. Potapov. *Materials*, **2020**, *13*, 2633. <https://doi.org/10.3390/ma13122699>
5. G. Lee, D. K. Yoo, I. Ahmed, H. J. Lee, and S. H. Jhung. *Chem. Eng. J.*, **2023**, *451*, 138538. <https://doi.org/10.1016/j.cej.2022.138538>
6. D. N. Dybtsev and K. P. Bryliakov. *Coord. Chem. Rev.*, **2021**, *437*, 213845. <https://doi.org/10.1016/j.ccr.2021.213845>

7. M. A. Agafonov, E. V. Alexandrov, N. A. Artyukhova, G. E. Bekmukhamedov, V. A. Blatov, V. V. Butova, Y. M. Gayfulin, A. A. Garibyan, Z. N. Gafurov, Yu. G. Gorbunova, L. G. Gordeeva, M. S. Gruzdev, A. N. Gusev, G. L. Denisov, D. N. Dybtsev, Yu. Yu. Enakieva, A. A. Kagilev, A. O. Kantyukov, M. A. Kiskin, K. A. Kovalenko, A. M. Kolker, D. I. Kolokolov, Y. M. Litvinova, A. A. Lysova, N. V. Maksimchuk, Y. V. Mironov, Yu. V. Nelyubina, V. V. Novikov, V. I. Ovcharenko, A. V. Piskunov, D. M. Polyukhov, V. A. Polyakov, V. G. Ponomareva, A. S. Poryvaev, G. V. Romanenko, A. V. Soldatov, M. V. Solovyeva, A. G. Stepanov, I. V. Terekhova, O. Yu. Trofimova, V. P. Fedin, M. V. Fedin, O. A. Kholdeeva, A. Yu. Tsivadze, U. V. Chervonova, A. I. Cherevko, V. F. Shul'gin, E. S. Shutova, and D. G. Yakhvarov. *J. Struct. Chem.*, **2022**, 63(5), 671. <https://doi.org/10.1134/S0022476622050018>
8. W.-J. Gu, J.-Z. Gu, M. V. Kirillova, and A. M. Kirillov. *CrystEngComm*, **2022**, 24, 5297. <https://doi.org/10.1039/D2CE00722C>
9. J. Gu, M. Wen, X. Liang, Z. Shi, M. Kirillova, and A. Kirillov. *Crystals*, **2018**, 8, 83. <https://doi.org/10.3390/cryst8020083>
10. Z. Yang, T. Hashimoto, R. Oketani, T. Nakamura, and I. Hisaki. *Chem. – Eur. J.*, **2022**, 28, e202201571. <https://doi.org/10.1002/chem.202201571>
11. B. N. Bhadra, I. Ahmed, H. J. Lee, and S. H. Jung. *Coord. Chem. Rev.*, **2022**, 450, 214237. <https://doi.org/10.1016/j.ccr.2021.214237>
12. Y. Zhao and D. Li. *J. Mater. Chem. C*, **2020**, 8, 12739. <https://doi.org/10.1039/d0tc03430d>
13. C. Yin, Q. Huang, G. Zhu, L. Liu, S. Li, X. Yang, and S. Wang. *J. Colloid Interface Sci.*, **2022**, 607, 1762. <https://doi.org/10.1016/j.jcis.2021.09.108>
14. I. Aswin Kumar, A. Jeyaseelan, N. Viswanathan, M. Naushad, and A. J. M. Valente. *J. Solid State Chem.*, **2021**, 302, 122446. <https://doi.org/10.1016/j.jssc.2021.122446>
15. Q. He, H. Zhao, Z. Teng, Y. Wang, M. Li, and M. R. Hoffmann. *Chemosphere*, **2022**, 303, 134987. <https://doi.org/10.1016/j.chemosphere.2022.134987>
16. F. M. Amombo Noa, E. S. Grape, M. Åhlén, W. E. Reinholdsson, C. R. Göb, F. X. Coudert, O. Cheung, A. K. Inge, and L. Öhrström. *J. Am. Chem. Soc.*, **2022**, 144, 8725. <https://doi.org/10.1021/jacs.2c02351>
17. Y. Zhang, Z. Gao, W. Liu, G. Liu, M. Zhu, S. Wu, W. Yao, and E. Gao. *Inorg. Chem. Commun.*, **2021**, 134, 109017. <https://doi.org/10.1016/j.inoche.2021.109017>
18. CrysAlisPro, Version 1.171.34.49. Agilent Technologies, **2011**.
19. O. V. Dolomanov, L. J. Bourhis, R. J. Gildea, J. A. K. Howard, and H. Puschmann. *J. Appl. Crystallogr.*, **2009**, 42, 339. <https://doi.org/10.1107/S0021889808042726>
20. P. Alemany, D. Casanova, S. Alvarez, C. Dryzun, and D. Avnir. Continuous Symmetry Measures: A New Tool in Quantum Chemistry. In: Reviews in Computational Chemistry, Vol. 30 / Eds. A. L. Parrill and K. B. Lipkowitz. John Wiley & Sons, **2017**, 289. <https://doi.org/10.1002/9781119356059.ch7>
21. A. Ruiz-Martínez, D. Casanova, and S. Alvarez. *Chem. – A Eur. J.*, **2008**, 14, 1291. <https://doi.org/10.1002/chem.200701137>
22. Y. Wan, J. Wang, H. Shu, B. Cheng, Z. He, P. Wang, and X. Tifeng. *Inorg. Chem.*, **2021**, 60, 7345. <https://doi.org/10.1021/acs.inorgchem.1c00502>
23. S. Dang, J.-H. Zhang, Z.-M. Sun, and H. Zhang. *Chem. Commun.*, **2012**, 48, 11139. <https://doi.org/10.1039/C2CC35432B>
24. P. A. Demakov, A. A. Ryadun, and V. P. Fedin. *Inorganics*, **2022**, 10, 163. <https://doi.org/10.3390/inorganics10100163>
25. Z.-Y. Fu, S.-M. Hu, W.-X. Du, J.-J. Zhang, S.-C. Xiang, and X.-T. Wu. *Jiegou Huaxue (1982-2004)*, **2004**, 23, 176. <https://chemport-n.cas.org/chemport-n/?APP=ftslink&action=reflink&origin=npq&version=1.0&coi=1%3ACAS%3A528%3ADC%2BD2cXit12qsrg%3D&md5=89fc042d539db70bcf425ce9770ff6fc>
26. J. Zhang, J. T. Bu, S. Chen, T. Wu, S. Zheng, Y. Chen, R. A. Nieto, P. Feng, and X. Bu. *Angew. Chem., Int. Ed.*, **2010**, 49, 8876. <https://doi.org/10.1002/anie.201003900>



27. P. A. Demakov, A. S. Bogomyakov, A. S. Urlukov, A. Y. Andreeva, D. G. Samsonenko, D. N. Dybtsev, and V. P. Fedin. *Materials*, **2020**, *13*, 486. <https://doi.org/10.3390/ma13020486>
28. Z.-H. Wang, J. Fan, and W.-G. Zhang. *Z. Anorg. Allg. Chem.*, **2009**, *635*, 2333. <https://doi.org/10.1002/zaac.200801412>